Int J Wireless Inf Networks (2009) 16:197–208
DOI 10.1007/s10776-009-0108-y

Doppler Spread Estimation for Broadband Wireless OFDM Systems Over Rician Fading Channels

Jun Tao · Jingxian Wu · Chengshan Xiao

Published online: 27 October 2009

Abstract In this paper, we present a new Doppler spread estimation algorithm for broadband wireless orthogonal frequency division multiplexing (OFDM) systems with fast time-varying and frequency-selective Rayleigh or Rician fading channels. The new algorithm is developed by analyzing the statistical properties of the power of the received OFDM signal in the time domain, thus it is not affected by the influence of frequency-domain inter-carrier interference (ICI) introduced by channel variation within one OFDM symbol. The operation of the algorithm doesn't require the knowledge of fading channel coefficients, transmitted data, or signal-to-noise ratio (SNR) at the receiver. It is robust against additive noise, and can provide accurate Doppler spread estimation with SNR as low as 0 dB. Moreover, unlike existing algorithms, the proposed algorithm takes into account the inter-tap correlation of the discrete-time channel representation, as is the case in practical systems. Simulation results demonstrate that this new algorithm can accurately estimate a wide range of Doppler spread with low estimation latency and high computational efficiency.

J. Tao
Department of Electrical and Computer Engineering, University of Missouri, Columbia, MO 65211, USA
e-mail: jtb84@mail.missouri.edu

J. Wu
Department of Electrical Engineering, University of Arkansas, Fayetteville, AR 72701, USA
e-mail: wuj@uark.edu

C. Xiao (✉)
Department of Electrical and Computer Engineering, Missouri University of Science and Technology, Rolla, MO 65409, USA
e-mail: xiaoc@mst.edu

Keywords Auto-covariance · Doppler spread estimation · OFDM

1 Introduction

Orthogonal frequency division multiplexing (OFDM) has become the dominant information transmission technique for a number of current and future wireless communication systems [1–5]. OFDM is designed primarily for system with quasi-static fading, i.e., the channel keeps constant during at least one symbol duration. To meet the ever increasing demand for broadband pervasive communications, OFDM systems designed for future wireless communications are expected to operate in an environment with high data transmission rate, high mobility, and high carrier frequency. High speed broadband communication dictates an operating environment of fast time-varying and frequency-selective fading. Fast time-varying fading introduces Doppler spread, which destroys the orthogonality among subcarriers in OFDM and causes inter-carrier interference (ICI), which is one of the main performance degrading factors for OFDM systems [6–8].

On the other hand, Doppler spread contains information about the key statistics of the wireless channel, and it provides important guidance for system design. Doppler spread has been utilized in single carrier systems for adaptive handoff algorithm [9], energy-efficient routing for mobile ad hoc networks [10], mobility and resource management for wireless multimedia networks [11], trajectory prediction for wireless networks with mobile base stations [12]. It has also been used in OFDM-based communication systems for adaptive channel estimation [13, 14], adaptive power control [15], and adaptive modulation and coding (AMC) [16]. Therefore, a good estimation of Doppler

spread is important for the design and implementation of practical wireless communication systems.

Doppler spread estimation has received extensive attentions for single carrier communication systems [17–26]. However, there are very limited works on Doppler spread estimation for OFDM systems [27, 28, 29, 30]. The Doppler spread estimation algorithms presented in [27] and [28] require the knowledge of the channel state information, which is usually difficult to extract, especially at high Doppler spread and low signal-to-noise ratio (SNR). The Doppler spread estimation in these works are performed by evaluating the auto-correlation functions of the frequency-domain signal [27] and the time-domain signal [28] at pilot tones. Since pilot tones only account for a small percentage of transmitted signals, a large number of OFDM blocks are required to extract the necessary channel statistics. In addition, the performance of the algorithm in [27] is negatively affected by ICI due to its frequency-domain operation. In [29], Doppler spread is estimated by extracting the correlation between cyclic prefix (CP) and its data counterpart within one OFDM symbol. Only the portion of the CP that has not been corrupted by inter-symbol interference (ISI) can be used for estimation. Since the uncontaminated part of the CP might be very small, especially when the delay spread of the channel is large, the applicability of the method in practical systems is limited. In addition, it is pointed out in [28] that the estimation accuracy of the CP-based algorithm degrades significantly at low SNR. All of these works assume a simplified discrete-time tapped-delay-line channel model with uncorrelated channel coefficients. It has been shown in [31] and [32] that the channel taps of equivalent discrete-time representation of the fading channel are actually correlated due to the time span of the transmit filter and the receive filter, and this correlation information is important for system design and evaluation. Furthermore, to the best of our knowledge, all existing algorithms are designed primarily for Rayleigh fading channels and they are unable to provide satisfactory Doppler spread estimation for frequency-selective Rician fading channel.

In this paper, a new Doppler spread estimation algorithm that does not suffer from any of the aforementioned limitations is proposed for broadband OFDM systems operating under doubly-selective (time-selective and frequency-selective) Rayleigh and Rician fading channels. The estimation is performed by collecting statistics from all the received time-domain signals. Unlike previous methods, the new algorithm does not require pilot symbols, and can operate at the presence of both unknown channel coefficients and unknown data symbols. It is robust to ICI and additive noise, and can provide accurate estimation of the Doppler spread even when the SNR is as low as 0 dB. In addition, the channel tap correlation of the equivalent discrete-time system representation is considered during the development of the algorithm. Simulation results show that the new algorithm provides accurate and high-efficiency estimation of the Doppler spread over a wide range of system configurations.

The remainder of this paper is organized as follows. Section 2 presents the discrete-time model of the OFDM system and preliminary statistical properties of the channel. In Sect. 3, the key statistics of the received time-domain signal are investigated, and the results are used to facilitate the development of the Doppler spread estimation algorithm. Based on the theoretical results in Sect. 3, a practical high-efficiency low-latency Doppler spread estimation algorithm is developed in Sect. 4. Simulation results are presented in Sect. 5, and Sect. 6 concludes the paper.

2 System Model and Assumptions

Consider an OFDM system with a block diagram shown in Fig. 1. For the ith $(i \in \mathbb{Z}^+)$ OFDM symbol, a set of N modulated symbols, $\boldsymbol{s}^{(i)} = [s_0^{(i)}, \ldots, s_{N-1}^{(i)}]^T \in \mathcal{S}^{N\times 1}$, with $\mathcal{S}$ being the modulation alphabet and $(\cdot)^T$ denoting the transpose operator, are multiplexed onto N orthonormal subcarriers, and the obtained time-domain samples, $x^{(i)}(n)$, can be expressed as

$$x^{(i)}(n) = \frac{1}{\sqrt{N}} \sum_{k=0}^{N-1} s_k^{(i)} e^{j\frac{2\pi}{N}kn}, -N_p \le n < N + N_q \tag{1}$$

where N_p and N_q are the lengths of cyclic prefix and cyclic postfix, respectively. Cyclic prefix and postfix are used to remove the ISI introduced by the causal part and non-causal part of the equivalent channel [32].

The modulated complex symbols, $s_k^{(i)}$, are assumed to be zero-mean complex random variables with independent real part and imaginary part, and the cross-correlation between two modulation symbols is

$$\mathbb{E}\left\{ s_{k_1}^{(i)} \left[s_{k_2}^{(j)} \right]^* \right\} = \delta(k_1 - k_2)\delta(i - j) \tag{2}$$

where $\mathbb{E}\{\cdot\}$ represents the operation of mathematical expectation, $\delta(\cdot)$ is the Kronecker delta function, and $(\cdot)^*$ stands for complex conjugate. The assumption is valid for a wide range of modulation schemes such as M-ary phase shift keying (MPSK), M-ary quadrature amplitude modulation (MQAM), etc.

The time-domain samples, $x^{(i)}(n)$, are passed through a transmit filter, $p_T(\tau)$, and then transmitted over the time-varying physical fading channel with impulse reponsse $g_c(t, \tau)$. At the receiver, the received time-domain signal is

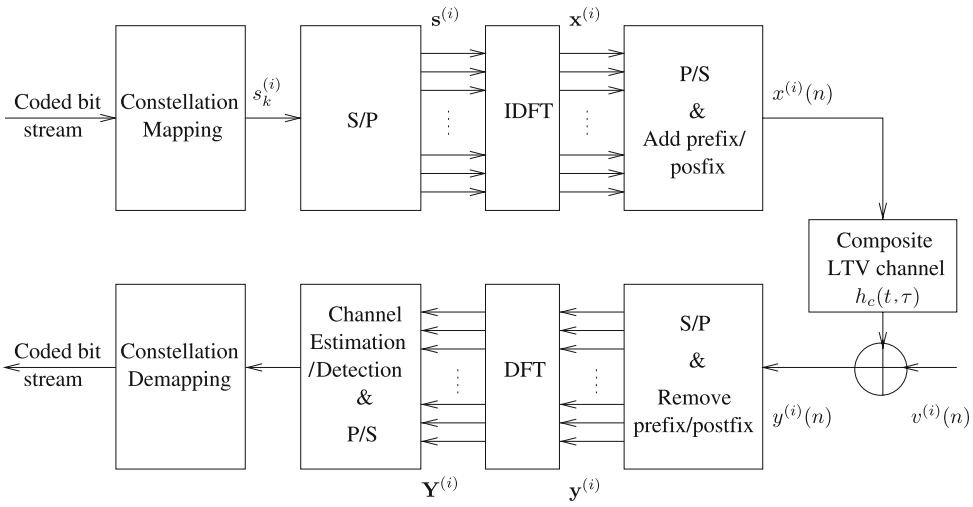

Fig. 1 OFDM system model (only $y^{(i)}(n)$ is used during Doppler spread estimation)

passed through a receive filter, $p_R(\tau)$. Define the continuous-time composite channel impulse response (CIR) as

$$h_c(t,\tau) = p_T(\tau) \otimes g_c(t,\tau) \otimes p_R(\tau) \tag{3}$$

where $a(\tau) \otimes b(t,\tau) = \int b(t,\alpha)a(\tau-\alpha)d\alpha$ represents convolution of time-varying signals. For system experiencing Rician fading, the physical channel $g_c(t, \tau)$ can be modeled as [33]

$$g_c(t,\tau) = \frac{g(t,\tau)}{\sqrt{1+K}} + \sqrt{\frac{K}{1+K}} h_{LOS}(t)\delta(\tau) \tag{4}$$

where K is the Rice factor, $g(t, \tau)$ is wide-sense stationary uncorrelated scattering (WSSUS) [34] Rayleigh fading component with normalized unit energy, and the line-of-sight (LOS) component is expressed by $h_{LOS}(t) = \exp(j2\pi f_d t\cos\theta_0 + j\phi_0)$ with f_d being the maximum Doppler spread, and θ_0 and ϕ_0 being the angle of arrival and the initial phase, respectively. It's assumed that θ_0 and ϕ_0 are uniformly distributed over $(-\pi, \pi]$.

At the receiver, the output of the receive filter is sampled at a rate of $1/T_s$, where T_s is the symbol period. After the removal of cyclic prefix and cyclic postfix, the received time-domain samples can be represented as [32]

$$y^{(i)}(n) = \frac{1}{\sqrt{1+K}} \sum_{l=-L_1}^{L_2} h^{(i)}(n,l)x^{(i)}(n-l) + \sqrt{\frac{K}{1+K}} h_{LOS}^{(i)}(n) \sum_{p=-P_1}^{P_2} \rho_p x^{(i)}(n-p) + v^{(i)}(n) \tag{5}$$

where $y^{(i)}(n) \triangleq y(((i-1)N_s+n)T_s)$ is the nth sample of the ith received OFDM symbol, with $n = 0, 1, \ldots, N-1$, and $N_s = N_p + N + N_q$ is the number of samples within one OFDM symbol including the prefix and postfix. The additive white Gaussian noise (AWGN) sample $v^{(i)}(n)$ has zero mean and variance σ^2. The channel coefficients, $\{h^{(i)}(n,l) \triangleq h(((i-1)N_s+n)T_s, lT_s)\}_{l=-L_1}^{L_2}$, are the discrete-time version of the continuous-time non-line-of-sight (NLOS) component $h(t,\tau) = p_R(\tau) \otimes g(t,\tau) \otimes p_T(\tau)$, with the non-negative integers, L_1 and L_2 determined by the transmit filter, receive filter, and channel power delay profile (PDP) [32]. The discrete-time version of the LOS component is denoted by $h_{LOS}^{(i)}(n) \triangleq h_{LOS}(((i-1)N_s + n)T_s)$. The effects of the transmit filter and receive filter on the LOS component is contained in the coefficient, $\rho_p = \int_{-\infty}^{\infty} p_T(s)p_R(pT_s - s)ds$, for $p = -P_1, \ldots, P_2$, with the non-negative integers P_1 and P_2 determined by the transmit and receive filters. For energy normalized transmit and receive filters, we have $\sum_{p=-P_1}^{P_2} \rho_p^2 = 1$. Specifically, $\rho_p = \delta(p)$ for filters satisfying Nyquist criterion. It should be noted that, with the insertion of cyclic prefix and postfix, the signal samples, $\{y^{(i)}(n)\}_{n=0}^{N-1}$, contains information contributed only from $\{x^{(i)}(n)\}_{n=0}^{N-1}$ of the ith transmitted OFDM symbol.

Due to the time span of the transmit filter and the receive filter, the discrete-time NLOS channel is generally non-causal, and the channel coefficients $\{h^{(i)}(n,l)\}_{l=-L_1}^{L_2}$ are mutually correlated across the delay-domain l, even though the underlying physical channel is causal and experiences uncorrelated scattering. The NLOS coefficients form a wide-sense stationary zero mean complex Gaussian random process with the auto-correlation function given by [32]

$$\mathbb{E}\{h^{(i_1)}(n_1,l_1)[h^{(i_2)}(n_2,l_2)]^*\} = C_{l_1,l_2} J_0\{2\pi f_d[(i_1-i_2)N_s + (n_1-n_2)]T_s\} \tag{6}$$

where C_{l_1,l_2} is the inter-tap correlation, $J_0(\cdot)$ is the zero-order Bessel function of the first kind, and f_d is the maximum Doppler spread. The value of C_{l_1,l_2} is determined by the transmit filter, the channel power delay profile, and the

receive filter. For energy normalized composite channel, we have $\sum_{l=-L_1}^{L_2} C_{l,l} = 1$.

3 Algorithm Development Based on Time-Domain Signal Statistics

In this section, theoretical analysis is performed to investigate the key second-order and fourth-order statistics of the received time-domain signal, $y^{(i)}(n)$, and the results are used to facilitate the development of the Doppler spread estimation algorithm.

3.1 Statistics of the Received Signals

Define the auto-correlation of the received time-domain signal, $y^{(i)}(n)$, and the auto-correlation of the received signal power, $|y^{(i)}(n)|^2$, as

$$R_{yy}(s,u,n,m) \triangleq \mathbb{E}\left\{ y^{(s+u)}(n+m)\left[y^{(s)}(n)\right]^* \right\} \tag{7a}$$

$$R_{|y|^2|y|^2}(s,u,n,m) \triangleq \mathbb{E}\left\{ |y^{(s+u)}(n+m)|^2 |y^{(s)}(n)|^2 \right\} \tag{7b}$$

where $s \in \mathbb{Z}^+$ and $u \in \mathbb{Z}$ are OFDM symbol index and index difference, and n and m are time instant and time lag in samples, respectively.

Substituting (1) and (5) into (7), we have the auto-correlations expressed in (8) and (9). It should be noted that the identities, $J_0[2\pi f_d(uN_s+m)T_s]\delta(u) = J_0(2\pi f_d m T_s)\delta(u)$, and $\cos[2\pi f_d(uN_s+m)T_s\cos\theta_0]\delta(u) = \cos(2\pi f_d m T_s\cos\theta_0)\delta(u)$, are used in the derivation of (8) and (9). The proofs for (8) and (9) are delegated to the Appendix. Observing (8) and (9) reveals that both $y(n)$ and $|y(n)|^2$ are wide-sense stationary since they are functions of the OFDM symbol index difference u and the time lag m, while independent of the starting OFDM symbol index s and the starting time instant n. Therefore, we denote $R_{yy}(s,u,n,m)$ by $R_{yy}(u,m)$ and $R_{|y|^2|y|^2}(s,u,n,m)$ by $R_{|y|^2|y|^2}(u,m)$ in the sequel unless specified otherwise.

$$\begin{aligned} R_{yy}(s,u,n,m) = \Bigg[& \frac{1}{N(1+K)} \sum_{l_1=-L_1}^{L_2} \sum_{l_2=-L_1}^{L_2} \sum_{k=0}^{N-1} C_{l_1,l_2} J_0(2\pi f_d m T_s) e^{j\frac{2\pi(l_2-l_1+m)k}{N}} \\ & + \frac{K}{N(1+K)} \sum_{p_1=-P_1}^{P_2} \sum_{p_2=-P_1}^{P_2} \sum_{k=0}^{N-1} \rho_{p_1}\rho_{p_2}^* \\ & \times e^{j2\pi f_d m T_s\cos\theta_0} e^{j\frac{2\pi(p_2-p_1+m)k}{N}} + \sigma^2\delta(m) \Bigg] \delta(u) \end{aligned} \tag{8}$$

$$\begin{aligned} & R_{|y|^2|y|^2}(s,u,n,m) = \\ & 1 + 2\sigma^2 + \sigma^4 + 2\sigma^2\delta(m)\delta(u) + \sigma^4\delta(m)\delta(u) \\ & + \frac{J_0^2[2\pi f_d(uN_s+m)T_s]}{(1+K)^2} \sum_{l_1=-L_1}^{L_2} \sum_{l_2=-L_1}^{L_2} |C_{l_1,l_2}|^2 \\ & + \frac{2KJ_0[2\pi f_d(uN_s+m)T_s]\cos[2\pi f_d(uN_s+m)T_s\cos\theta_0]}{(1+K)^2} \\ & \times \sum_{l_1=-L_1}^{L_2} \sum_{\substack{l_2=-L_1 \\ l_1=p_1, l_2=p_2}}^{L_2} \sum_{p_1=-P_1}^{P_2} \sum_{p_2=-P_1}^{P_2} C_{l_1,l_2}\rho_{p_1}^*\rho_{p_2} \\ & + \frac{1}{(1+K)^2N^2} \sum_{l_1=-L_1}^{L_2} \sum_{l_2=-L_1}^{L_2} \sum_{l_3=-L_1}^{L_2} \sum_{l_4=-L_1}^{L_2} \sum_{\substack{k_1=0 \\ k_1\neq k_2}}^{N-1} \sum_{k_2=0}^{N-1} \\ & \left[C_{l_1,l_2}C_{l_3,l_4} + C_{l_1,l_4}C_{l_2,l_3}^* J_0^2(2\pi f_d m T_s) \right] \\ & \times e^{j\frac{2\pi[k_1(m+l_4-l_1)-k_2(m+l_3-l_2)]}{N}}\delta(u) \\ & + \frac{K}{(1+K)^2N^2} \sum_{l_1=-L_1}^{L_2} \sum_{l_2=-L_1}^{L_2} \sum_{p_1=-P_1}^{P_2} \sum_{p_2=-P_1}^{P_2} \sum_{\substack{k_1=0 \\ k_1\neq k_2}}^{N-1} \sum_{k_2=0}^{N-1} C_{l_1,l_2}\rho_{p_1}\rho_{p_2}^* \\ & \times \left[e^{j\frac{2\pi[k_1(m-l_1+p_2)-k_2(m-l_2+p_1)]}{N}} + e^{j\frac{2\pi[k_1(m-p_1+l_2)-k_2(m-p_2+l_1)]}{N}} \right]\delta(u) \\ & + \frac{2KJ_0(2\pi f_d m T_s)\cos(2\pi f_d m T_s\cos\theta_0)}{(1+K)^2N^2} \\ & \sum_{l_1=-L_1}^{L_2} \sum_{l_2=-L_1}^{L_2} \sum_{p_1=-P_1}^{P_2} \sum_{p_2=-P_1}^{P_2} \sum_{\substack{k_1=0 \\ k_1\neq k_2}}^{N-1} \sum_{k_2=0}^{N-1} C_{l_1,l_2}\rho_{p_1}^*\rho_{p_2} \\ & \times e^{j\frac{2\pi[k_1(m+l_2-l_1)-k_2(m+p_2-p_1)]}{N}}\delta(u) \\ & + \frac{K^2}{(1+K)^2N^2} \sum_{p_1=-P_1}^{P_2} \sum_{p_2=-P_1}^{P_2} \sum_{p_3=-P_1}^{P_2} \sum_{p_4=-P_1}^{P_2} \sum_{\substack{k_1=0 \\ k_1\neq k_2}}^{N-1} \sum_{k_2=0}^{N-1} \\ & \rho_{p_1}\rho_{p_2}^*\rho_{p_3}\rho_{p_4}^* e^{j\frac{2\pi[k_1(m+p_4-p_1)-k_2(m+p_3-p_2)]}{N}}\delta(u). \end{aligned} \tag{9}$$

Setting $u=0, m=0$ in (8), we have $R_{yy}(0) \triangleq R_{yy}(u=0, m=0)$ as

$$\begin{aligned} R_{yy}(0) = & \frac{1}{N(1+K)} \sum_{l_1=-L_1}^{L_2} \sum_{l_2=-L_1}^{L_2} \sum_{k=0}^{N-1} C_{l_1,l_2} e^{j\frac{2\pi(l_2-l_1)k}{N}} \\ & + \frac{K}{N(1+K)} \sum_{p_1=-P_1}^{P_2} \sum_{p_2=-P_1}^{P_2} \sum_{k=0}^{N-1} \sigma_{p_1}\sigma_{p_2}^* e^{j\frac{2\pi(p_2-p_1)k}{N}} + \sigma^2 \\ = & 1 + \sigma^2. \end{aligned} \tag{10}$$

Thus, the auto-covariance of the received signal power can be written as

$$V_{|y|^2|y|^2}(u,m) = R_{|y|^2|y|^2}(u,m) - \mathbb{E}^2\left[\left|y^{(s)}(n)\right|^2\right] = R_{|y|^2|y|^2}(u,m) - (1+\sigma^2)^2. \tag{11}$$

The statistics described in (8), (9) and (11) are expressed as functions of the Doppler spread f_d. However, the expressions of the statistics are extremely complicated, thus it would be rather difficult, if not impossible, to directly extract the values of f_d based on these expressions. To facilitate the development of the Doppler spread estimation algorithm, we have the following three remarks on the signal statistics.

Remark 1 From (8), we observe that signals from different OFDM symbols, i.e., $u \neq 0$, are always uncorrelated regardless of the value of m. This observation is intuitive since signals within one OFDM symbol are independent from adjacent OFDM symbols due to the presence of cyclic prefix and cyclic postfix. For the case $u = 0$, the auto-correlation of the received signal samples within one OFDM symbol interval is also zero if $L < |m| < N - L$, where $L = L_1 + L_2$, , because both of the triple summation terms in (8) are zeros in this case. For other values of m, the value of $R_{yy}(u = 0, m)$ is involved with m in a very complicated way as evident in (8). Therefore, the auto-correlation function, $R_{yy}(u,m)$, is not a good candidate for Doppler spread estimation.

Remark 2 When $u \neq 0$, the auto-correlation and auto-covariance of the received signal power in (9) and (11) can be simplified as follows

$$\begin{aligned} R_{|y|^2|y|^2}(u,m) =& 1 + 2\sigma^2 + \sigma^4 + \frac{J_0^2[2\pi f_d(uN_s+m)T_s]}{(1+K)^2} \\ &\times \sum_{l_1=-L_1}^{L_2}\sum_{l_2=-L_1}^{L_2} |C_{l_1,l_2}|^2 \\ &+ \frac{2KJ_0[2\pi f_d(uN_s+m)T_s]\cos[2\pi f_d(uN_s+m)T_s\cos\theta_0]}{(1+K)^2} \\ &\times \sum_{\substack{l_1=-L_1 \\ l_1=p_1,l_2=p_2}}^{L_2}\sum_{l_2=-L_1}^{L_2}\sum_{p_1=-P_1}^{P_2}\sum_{p_2=-P_1}^{P_2} C_{l_1,l_2}\rho_{p_1}^*\rho_{p_2} \end{aligned} \tag{12}$$

$$\begin{aligned} V_{|y|^2|y|^2}(u,m) =& \frac{J_0^2[2\pi f_d(uN_s+m)T_s]}{(1+K)^2}\sum_{l_1=-L_1}^{L_2}\sum_{l_2=-L_1}^{L_2}|C_{l_1,l_2}|^2 \\ &+ \frac{2KJ_0[2\pi f_d(uN_s+m)T_s]\cos[2\pi f_d(uN_s+m)T_s\cos\theta_0]}{(1+K)^2} \\ &\times \sum_{\substack{l_1=-L_1 \\ l_1=p_1,l_2=p_2}}^{L_2}\sum_{l_2=-L_1}^{L_2}\sum_{p_1=-P_1}^{P_2}\sum_{p_2=-P_1}^{P_2} C_{l_1,l_2}\rho_{p_1}^*\rho_{p_2}. \end{aligned} \tag{13}$$

It is worth pointing out that the expression in (13) is independent of the AWGN variance σ^2.

Remark 3 Comparing (9) and (11) with (12) and (13), we can see that there are complicated extra terms involving f_d in the expressions of the auto-correlation and auto-covariance of the signal power when $u = 0$ as compared to the $u \neq 0$ case. Since it's extremely difficult to evaluate the extra terms, the $u = 0$ case is not a desirable candidate for Doppler spread estimation.

Based on the analysis above, we conclude that the auto-covariance of signal power evaluated at $u \neq 0$ is the most suitable candidate for Doppler spread estimation. Compared to other cases, $V_{|y|^2|y|^2}(u,m)$ at $u \neq 0$ has two advantages. First, it is directly related to the maximum Doppler spread in an expression that is easy to analyze. Second, the effect of AWGN is completely removed, and this is highly desirable for the design of a robust estimation algorithm.

3.2 Doppler Spread Estimation

We are now in a position to develop the Doppler spread estimation algorithm based on the auto-covariance given in (13). Denote

$$\alpha = \frac{1}{(1+K)^2}\sum_{l_1=-L_1}^{L_2}\sum_{l_2=-L_1}^{L_2}|C_{l_1,l_2}|^2, \tag{14a}$$

$$\beta = \frac{2K}{(1+K)^2}\sum_{l_1=-L_1}^{L_2}\sum_{\substack{l_2=-L_1 \\ l_1=p_1,l_2=p_2}}^{L_2}\sum_{p_1=-P_1}^{P_2}\sum_{p_2=-P_1}^{P_2} C_{l_1,l_2}\rho_{p_1}^*\rho_{p_2}, \tag{14b}$$

$$z = 2\pi f_d(uN_s+m)T_s, \tag{14c}$$

then (13) can be written in a compact form as

$$V_{|y|^2|y|^2}(z) = \alpha J_0^2(z) + \beta J_0(z)\cos(z\cos\theta_0). \tag{15}$$

Since the values of α and β are unknown, (15) cannot be used directly for the estimation of the Doppler spread f_d. Instead, we resort to the normalized auto-covariance defined as

$$V_N(g,z) \triangleq \frac{V_{|y|^2|y|^2}(gz)}{V_{|y|^2|y|^2}(z)} = \frac{\alpha J_0^2(gz) + \beta J_0(gz)\cos(gz\cos\theta_0)}{\alpha J_0^2(z) + \beta J_0(z)\cos(z\cos\theta_0)}, \quad (g > 1 \text{ integer}) \tag{16}$$

where the integer parameter g can be adjusted to achieve better estimation accuracy. When g is properly chosen such that gz is small, second-order approximations, $J_0(x) \approx 1 - x^2/4$ and $\cos(x) \approx 1 - x^2/2$, can be employed, and this leads to the following approximation

$$V_N(g,z) \approx \frac{\alpha[1-(gz)^2/4]^2 + \beta[1-(gz)^2/4][1-(gz\cos\theta_0)^2/2]}{\alpha(1-z^2/4)^2 + \beta(1-z^2/4)[1-(z\cos\theta_0)^2/2]}. \tag{17}$$

To further simplify the representation, replacing $\cos^2\theta_0$ with its expectation $\mathbb{E}\{\cos^2\theta_0\} = 0.5$, we are able to cancel the two unknown parameters, α and β, from the expression of $V_N(g, z)$, and the result is

$$V_N(g,z) \approx \frac{[1-(gz)^2/4]^2}{(1-z^2/4)^2}. \tag{18}$$

The solution of z from (18) is

$$z = 2\sqrt{\frac{1-U_N(g,z)}{g^2-U_N(g,z)}} \tag{19}$$

where $U_N(g,z) \triangleq \sqrt{V_N(g,z)}$. Let $u = 1$, $m = 0$, then $z = 2\pi f_d N_s T_s$, and the estimation of the Doppler spread is obtained as

$$\tilde{f}_d = \frac{\sqrt{\frac{1-U_N(g,z)}{g^2-U_N(g,z)}}}{\pi N_s T_s} = \frac{F_1(g,z)}{\pi N_s T_s} \tag{20}$$

where

$$F_1(g,z) \triangleq \sqrt{\frac{1-U_N(g,z)}{g^2-U_N(g,z)}}. \tag{21}$$

It should be noted that other values of u and m can also be used in Doppler spread estimation without affecting the estimation accuracy. In this paper, however, we fix $z = 2\pi f_d N_s T_s$ without loss of generality.

Similarly, if we employ fourth-order approximations: $J_0(x) \approx 1 - x^2/4 + x^4/64$ and $\cos(x) \approx 1 - x^2/2 + x^4/24$, and note the fact that $\mathbb{E}\{\cos^4\theta_0\} = \frac{3}{8}$, then

$$\begin{aligned} V_N(g,z) &\approx \frac{\alpha[1-(gz)^2/4+(gz)^4/64]^2 + \beta[1-(gz)^2/4+(gz)^4/64][1-(gz\cos\theta_0)^2/2+(gz\cos\theta_0)^4/24]}{\alpha(1-z^2/4+z^4/64)^2 + \beta(1-z^2/4+z^4/64)[1-(z\cos\theta_0)^2/2+(z\cos\theta_0)^4/24]} \\ &= \frac{[1-(gz)^2/4+(gz)^4/64]^2}{(1-z^2/4+z^4/64)^2}, \end{aligned} \tag{22}$$

from which z can be solved as

$$z = 2\sqrt{2}\sqrt{\frac{g^2-U_N(g,z)-(g^2-1)\sqrt{U_N(g,z)}}{g^4-U_N(g,z)}}. \tag{23}$$

The Doppler spread estimation using fourth-order approximation can then be obtained from (23) as

$$\hat{f}_d = \frac{\sqrt{2}\sqrt{\frac{g^2-U_N(g,z)-(g^2-1)\sqrt{U_N(g,z)}}{g^4-U_N(g,z)}}}{\pi N_s T_s} = \frac{F_2(g,z)}{\pi N_s T_s} \tag{24}$$

where

$$F_2(g,z) \triangleq \sqrt{2}\sqrt{\frac{g^2-U_N(g,z)-(g^2-1)\sqrt{U_N(g,z)}}{g^4-U_N(g,z)}}. \tag{25}$$

When an estimate of the Doppler spread is obtained, the mobile speed can be calculated from Doppler spread as $v = f_d c/f_c$, where c is the speed of light and f_c is the carrier frequency.

Compared to existing algorithms, the newly proposed method has the following advantages. First, the estimation of the Doppler spread doesn't require the knowledge of fading channel coefficients or transmitted data symbols. Thus, all of the received signals, including both unknown data and known pilot, can be used in the estimation. Second, the effect of additive noise is removed in the estimation process due to the employment of the auto-covariance of the received signal power. Third, the channel inter-tap correlation, which is present in practical systems, is taken into account during the estimation process. Fourth, the estimation is performed over time-domain signals, thus it is not affected by the ICI in frequency domain.

4 A Practical Doppler Estimation Algorithm

Based on the theoretical analysis presented in Sect. 3, a practical Doppler spread estimation algorithm with low estimation latency and high computation efficiency is presented in this section.

From the theoretical estimators given in (20) and (24), the proper operation of the Doppler estimation algorithm requires the knowledge of the auto-covariance function, $V_{|y|^2|y|^2}(u,m)$, which can be approximated using time average. To obtain an accurate time-averaged approximation of the auto-covariance function, long data sequences are needed. This will result in long estimation delay with high computational complexity. To keep the estimation latency small while achieve satisfactory estimation reliability, we pass the received signal power, $p^{(i)}(n) = |y^{(i)}(n)|^2$, through a low pass filter to suppress the effects of

AWGN and power fluctuations. The filtered signal power can be represented by

$$\hat{p}^{(i)}(n) = \sum_{l=0}^{L_f} f(l) p^{(i)}(n-l) \tag{26}$$

where L_f and $f(l)$ are the order and coefficient of the low pass filter, respectively.

The time-averaged approximation of the auto-covariance function can then be calculated by using the filtered signal power from M consecutive OFDM symbols, and the result is

$$\hat{V}_{|y|^2|y|^2}(u,m) = \frac{1}{(M-u)(N-m)} \sum_{i=1}^{M-u} \sum_{n=0}^{N-m-1} \times [\hat{p}^{(i+u)}(n+m) - \bar{p}][\hat{p}^{(i)}(n) - \bar{p}] \tag{27}$$

where $\bar{p} = \frac{1}{MN} \sum_{i=1}^{M} \sum_{n=0}^{N-1} \hat{p}^{(i)}(n)$ is the time average of the signal power.

In addition to the auto-covariance function, another key parameter required for Doppler spread estimation is the integer g as shown in (20) and (24). The selection of g depends on two factors: first, gz should be small such that approximations in (18) and (22) still hold; second, for a given Doppler spread f_d, or $z = 2\pi f_d N_s T_s$, the normalized auto-covariance, $V_N(g,z)$, should not be too close to 1, such that enough information can be collected from $V_N(g,z)$ for Doppler spread estimation. To meet both of the two objectives, the value of g should adapt roughly according to the variation of Doppler spread. Therefore, we classify the Doppler spread into three categories, "low", "medium", and "high", and different values of g are used for each of the three categories.

Classification of Doppler spread is performed at the receiver by using the normalized auto-covariance of the received signal power. In (11), when $u = 0$, we choose a value m such that $T_m = mT_s$ is less than 30 μs, then $J_0(2\pi f_d m T_s) \approx 1$ and $\cos(2\pi f_d m T_s \cos\theta_0) \approx 1$ even if f_d is as high as 500 Hz. In this case, the auto-covariance $V_{|y|^2|y|^2}(u=0,m)$ tends to a constant value irrelevant to f_d. We denote this constant as $V_{|y|^2|y|^2}(T_m)$. Further, choose $u = u_0$, such that $T_{blk} = u_0 T_{sym} \approx 5$ ms, where $T_{sym} = N_s T_s$ is the time duration of one OFDM symbol including cyclic prefix and postfix. Similarly, define $V_{|y|^2|y|^2}(T_{blk}) \triangleq V_{|y|^2|y|^2}(u = u_0, m = 0)$. Then, the classification of Doppler spread can be achieved as follows

$$\frac{V_{|y|^2|y|^2}(T_{blk})}{V_{|y|^2|y|^2}(T_m)} \begin{cases} > 0.95, & \text{low}, \\ < 0.3, & \text{high}, \\ \text{otherwise}, & \text{medium}. \end{cases} \tag{28}$$

where the classification thresholds, 0.95 and 0.3, are chosen for illustration purpose only. Other threshold values can be obtained through optimization for different levels of "low", "high", and "medium".

Based on the Doppler spread classification given in (28), the value of g corresponding to each category is

$$g = \begin{cases} 10u_0, & \text{low}, \\ u_0, & \text{medium}, \\ \lceil 0.1u_0 \rceil, & \text{high}. \end{cases} \tag{29}$$

The values used in (29) are obtained based on empirical simulation results.

With the approximated auto-covariance function in (27) and the values of g given in (29), the Doppler spread can be estimated by substituting (27) and (29) into (20) or (24) with second-order and fourth-order approximations, respectively. The practical Doppler spread estimation algorithm is summarized as follows.

Step 1. Choose $\{m, u_0, M\}$ such that $mT_s < 30\,\mu s$, $T_{blk} = u_0 T_{sym} \approx 5$ ms, and $MT_{sym} < 1$ s.
Step 2. Compute $V_{|y|^2|y|^2}(T_m)$ and $V_{|y|^2|y|^2}(T_{blk})$. Classify Doppler spread as "low", "medium" or "high" according to (28), and select g based on (29).
Step 3. Compute $\hat{V}_{|y|^2|y|^2}(z)$ and $\hat{V}_{|y|^2|y|^2}(gz)$ with different values of g from (29), then obtain Doppler spread estimations $\tilde{f}_d$ and $\hat{f}_d$ according to (20) and (24) as follows:

$$\tilde{f}_d = \begin{cases} \frac{F_1(10u_0,z)}{\pi N_s T_s}, & \text{low}, \\ \frac{F_1(u_0,z)}{\pi N_s T_s}, & \text{medium}, \\ \frac{F_1(\lceil 0.1u_0 \rceil,z)}{\pi N_s T_s}, & \text{high}. \end{cases} \tag{30}$$

$$\hat{f}_d = \begin{cases} \frac{F_2(10u_0,z)}{\pi N_s T_s}, & \text{low}, \\ \frac{F_2(u_0,z)}{\pi N_s T_s}, & \text{medium}, \\ \frac{F_2(\lceil 0.1u_0 \rceil,z)}{\pi N_s T_s}, & \text{high}. \end{cases} \tag{31}$$

Step 4. Take the average of $\tilde{f}_d$ and $\hat{f}_d$ in (30) and (31) as the final Doppler spread estimation $\bar{f}_d = (\hat{f}_d + \tilde{f}_d)/2$.

5 Simulation

In this section, the performance of the proposed Doppler spread estimation algorithm is evaluated by performing simulations in a DVB-H system [2].

In the simulation, one OFDM symbol excluding cyclic prefix and postfix has a time duration of $T_u = 224$ μs. Sampling interval is $T_s = T_u/N$, where the value of N is 2048 corresponding to the 2K-mode of DVB-H system. The lengths of the cyclic prefix and cyclic postfix are set as $N_p = N_q = N/8 = 256$. One OFDM frame consists of 68 OFDM symbols, and four frames form one super-frame. The transmit filter, $p_T(\tau)$, and the receive filter, $p_R(\tau)$, are normalized square root raised cosine filter with roll-off

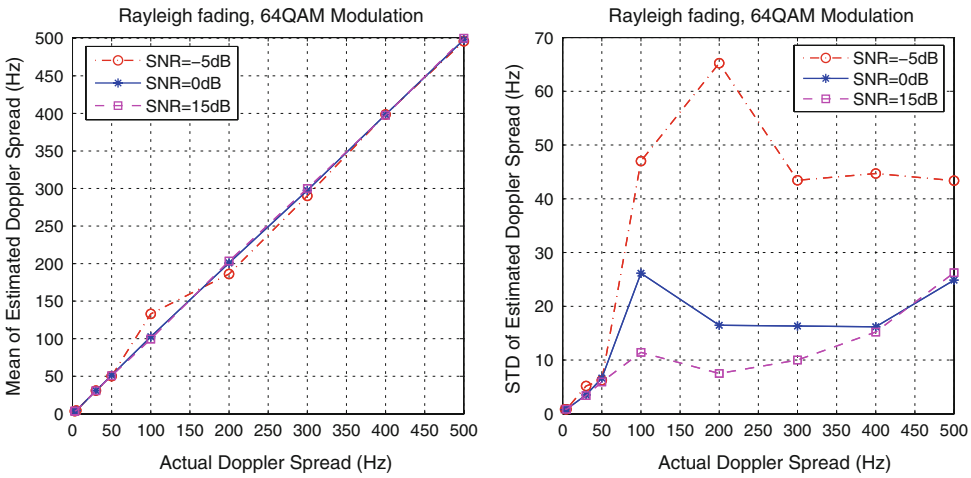

Fig. 2 Doppler spread estimation for frequency-selective Rayleigh fading channel with 64QAM modulation

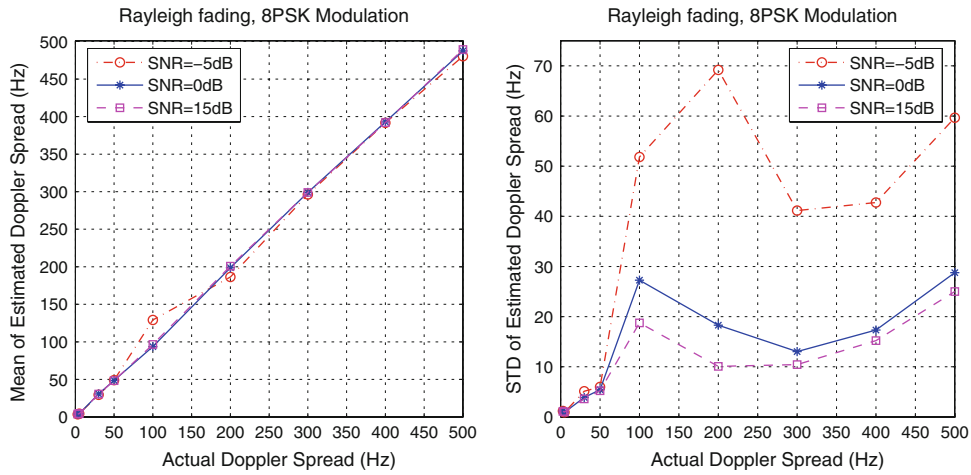

Fig. 3 Doppler spread estimation for frequency-selective Rayleigh fading channel with 8PSK modulation

factor 0.3. The power delay profile of the wireless physical fading channel has 120 uncorrelated taps with tap space being $T_s/2$. The average power of the first 40 taps ramps up linearly and the last 80 taps ramps down linearly. The equivalent T_s-spaced composite discrete-time channel, $h(n, l)$, has 63 *correlated* taps. The noise-suppression low pass filter has 50 taps, and $u_0 = 20$ is selected in (29) based on the above system configuration.

We first study the estimation performance in Rayleigh fading channel with Rice factor $K = 0$. The mean and standard deviation of the estimated Doppler spreads obtained with the proposed algorithm are shown in Fig. 2 for a system with 64QAM modulation. For each Doppler spread, the estimation is performed over $N_f = 24$ consecutive OFDM frames, which correspond to a time duration less than 0.5 s. It's clear from the figure that the proposed algorithm provides accurate and reliable estimation of the Doppler spread for SNR as low as 0 dB. More accurate estimations can be achieved at higher SNR. Similar observation is obtained for system with 8PSK modulation as shown in Fig. 3, which is obtained by using the same parameters as in Fig. 2 except the modulation scheme. Comparing Figs. 2 and 3, we conclude that the proposed estimation algorithm is insensitive to modulation schemes.

In Fig. 4, the normalized standard deviations of the estimated Doppler spreads are plotted as a function of the number of OFDM frames, N_f, used in one estimation. It is clearly shown that the standard deviations are within 10% of the true Doppler spreads. As expected, the estimation standard deviation decreases when more OFDM frames are used during the estimation. This is intuitive because more frames lead to a better time-averaged approximation of the auto-covariance function.

The simulation results for Rician fading with 64QAM modulation are presented in Fig. 5. The Rice factor is fixed at $K = 5$, and the Rician channel simulator in [33] is used for the generation of Rician fading during simulation. Comparing the results in Figs. 2 and 5, we can see that the estimation accuracy in Rician fading channel is slightly worse compared to the Rayleigh case. The performance degradation is mainly caused by the approximations of $\cos(x)$ and $\cos^2(\theta_0)$ used in the derivation of (18) and (22)

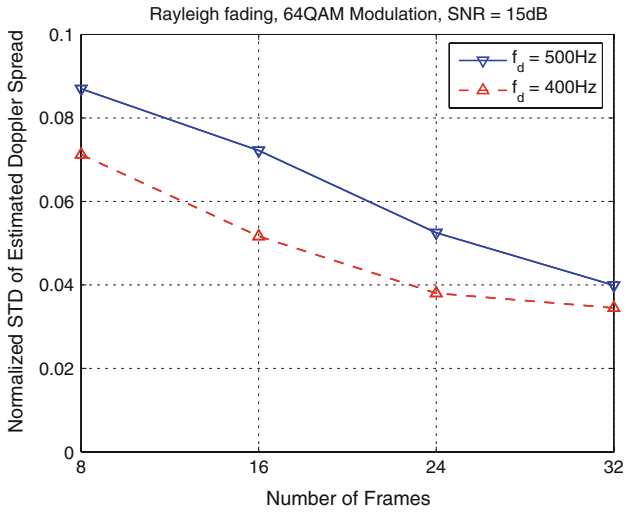

Fig. 4 Normalized standard deviation of estimated Doppler v.s. number of OFDM frames used in estimation for Rayleigh fading channel with 64QAM modulation

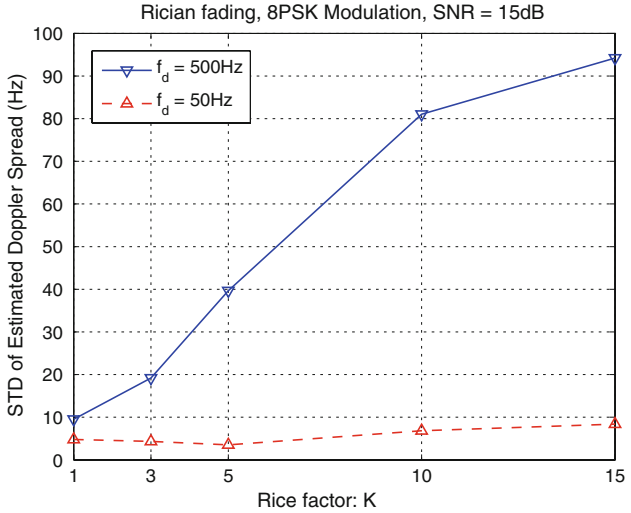

Fig. 6 Standard deviation of estimated Doppler v.s. Rice factor K with 8PSK modulation

for Rician fading channel. Such approximations are not required in Rayleigh fading channel. Even though the estimation accuracy in Rician fading channel is slightly worse compared to the Rayleigh case, the algorithm can still obtain a very accurate estimation of the Doppler spread and the estimation accuracy improves with the increase of SNR, as expected. Similar results are obtained for other modulation schemes and this corroborates that the proposed method is insensitive to modulation schemes.

The impact of Rice factor on the performance of the estimation algorithm is investigated in Fig. 6, where the standard deviation of the estimated Doppler spread is shown as a function of Rice factor K at different values of the Doppler spread. Systems with 8PSK modulation are used in this example. It can be seen from the figure that the estimation accuracy degrades as K increases. As analyzed before, the performance degradation is mainly due to extra approximations involved in the LOS component of the fading during the estimation process.

6 Conclusions

An accurate low-latency Doppler spread estimation algorithm was presented in this paper for OFDM systems with fast time-varying frequency-selective Rayleigh and Rician fading. The algorithm doesn't require pilots in the transmitted signal, and was developed by analyzing the statistical properties of received signals containing unknown transmitted data symbols and unknown channel fading. The estimation was performed with the auto-covariance function of the power of the received time-domain signals. Since the algorithm operates in the time domain, its

Fig. 5 Doppler spread estimation for frequency-selective Rician fading channel with 64QAM modulation

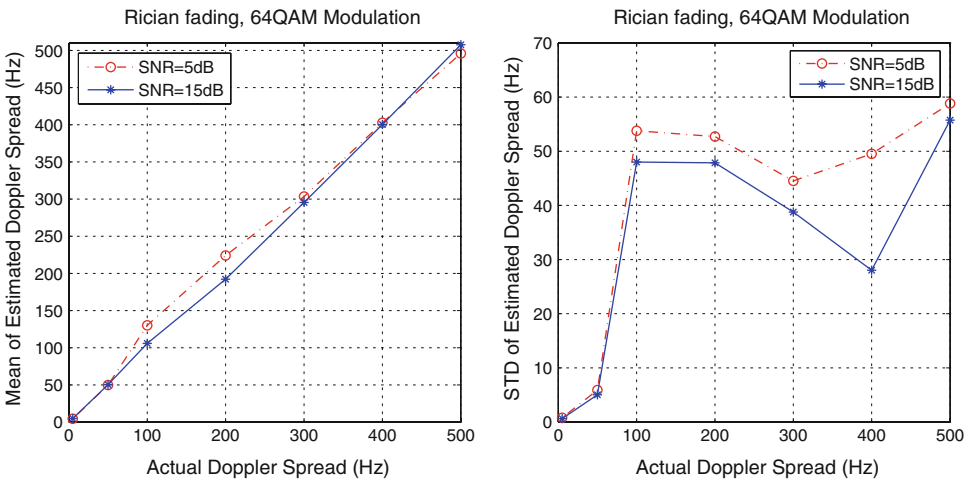

performance is not affected by the ICI in the frequency domain. In addition, a practical algorithm was proposed for accurate and high-efficiency Doppler spread estimation. Extensive simulations have shown that the new algorithm works well for doubly-selective Rayleigh and Rician fading channels at SNR as low as 0 dB.

Acknowledgement This work was supported in part by the National Science Foundation under Grants CCF-0832833, CCF-0915846 and ECCS-0917041.

Appendix

Proof of (8) and (9)

The auto-correlation function of the received time-domain OFDM signal is calculated as

$$
\begin{aligned}
R_{yy}(s,u,n,m) &= \mathbb{E}\left\{ y^{(s+u)}(n+m)\left[y^{(s)}(n)\right]^* \right\} \\
&= \mathbb{E}\left\{ \left[\frac{1}{\sqrt{1+K}} \sum_{l_1=-L_1}^{L_2} h^{(s+u)}(n+m,l_1)x^{(s+u)}(n+m-l_1) + \sqrt{\frac{K}{1+K}} h_{LOS}^{(s+u)}(n+m) \sum_{p_1=-P_1}^{P_2} \sigma_{p_1} x^{(s+u)}(n+m-p_1) \right.\right. \\
&\quad \left.\left. + v^{(s+u)}(n+m) \right] \times \left[\frac{1}{\sqrt{1+K}} \sum_{l_2=-L_1}^{L_2} h^{(s)}(n,l_2)x^{(s)}(n-l_2) + \sqrt{\frac{K}{1+K}} h_{LOS}^{(s)}(n) \sum_{p_2=-P_1}^{P_2} \sigma_{p_2} x^{(s)}(n-p_2) + v^{(s)}(n) \right]^* \right\} \\
&= \frac{1}{1+K} \sum_{l_1=-L_1}^{L_2} \sum_{l_2=-L_1}^{L_2} \mathbb{E}\left\{ h^{(s+u)}(n+m,l_1)\left[h^{(s)}(n,l_2)\right]^* x^{(s+u)}(n+m-l_1)\left[x^{(s)}(n-l_2)\right]^* \right\} \\
&\quad + \frac{K}{1+K} \sum_{p_1=-P_1}^{P_2} \sum_{p_2=-P_1}^{P_2} \sigma_{p_1}\sigma_{p_2}^* \mathbb{E}\left\{ h_{LOS}^{(s+u)}(n+m)\left[h_{LOS}^{(s)}(n)\right]^* x^{(s+u)}(n+m-p_1)\left[x^{(s)}(n-p_2)\right]^* \right\} \\
&\quad + \mathbb{E}\left\{ v^{(s+u)}(n+m)\left[v^{(s)}(n)\right]^* \right\} \\
&= \left[\frac{1}{N(1+K)} \sum_{l_1=-L_1}^{L_2} \sum_{l_2=-L_1}^{L_2} \sum_{k=0}^{N-1} C_{l_1,l_2} J_0(2\pi f_d m T_s) e^{j\frac{2\pi(l_2-l_1+m)k}{N}} \right. \\
&\quad \left. + \frac{K}{N(1+K)} \sum_{p_1=-P_1}^{P_2} \sum_{p_2=-P_1}^{P_2} \sum_{k=0}^{N-1} \sigma_{p_1}\sigma_{p_2}^* e^{j2\pi f_d m T_s \cos\theta_0} e^{j\frac{2\pi(p_2-p_1+m)k}{N}} + \sigma^2\delta(m) \right] \delta(u)
\end{aligned} \tag{32}
$$

where $x^{(i)}(n)$ defined in (1) is used in the derivation of the last equality, thus (8) is proved.

The proof of Eq. 9 relies on the following two identities: $\mathbb{E}\{v_1v_2v_3\} = 0$ and $\mathbb{E}\{v_1v_2v_3v_4\} = \mathbb{E}\{v_1v_2\}\mathbb{E}\{v_3v_4\} + \mathbb{E}\{v_1v_3\}\mathbb{E}\{v_2v_4\} + \mathbb{E}\{v_1v_4\}\mathbb{E}\{v_2v_3\}$, where v_1, v_2, v_3 and v_4 are zero-mean Gaussian random variables. With the above identities, (9) can be derived based on the definition of auto-covariance function. The derivation process is extremely lengthy and tedious, but straightforward, thus the details are omitted here for brevity.

References

1. IEEE Standard for Wireless LAN Medium Access Control (MAC) and Physical Layer (PHY) Specifications, IEEE Std. 802.11g-2003, June 2003.
2. Digital Video Broadcasting (DVB): Transmission System for Handheld Terminals (DVB-H), ETSI Std. EN 302 304, Nov. 2004.
3. IEEE Standard for Local and Metropolitan Area Networks—Part 16: Air Interface for Fixed and Mobile Broadband Wireless Access Systems, IEEE Std. 802.16e-2006, Feb. 2006.
4. T. Zahariadis, Trends in the path to 4G, *IEEE Communincation Engineering*, Vol. 14, No. 1, pp. 12–15, 2003.
5. R. Prasad, *OFDM for Wireless Communication Systems*, Artech House, 2004.
6. A. Stamoulis, S. N. Diggavi, and N. Al-Dhahir, Intercarrier interference in MIMO OFDM, *IEEE Transactions on Signal Processing*, Vol. 50, No. 10, pp. 2451–2464, 2002.
7. M. Speth, S. A. Fechtel, G. Fock, and H. Meyr, Optimum receiver design for wireless broad-band systems using OFDM–Part I, *IEEE Transactions on Communications*, Vol. 47, No. 11, pp. 1668–1677, 1999.
8. P. Schniter, Low-complexity equalization of OFDM in doubly selective channels, *IEEE Transactions on Signal Processing*, Vol. 52, No. 4, pp. 1002–1011, 2004.
9. C. Tepedelenlioglu, A. Abdi, G. Giannakis, and M. Kaveh, Estimation of Doppler spread and signal strength in mobile communications with applications to handoff and adaptive transmission, *Wireless Commnunication and Mobile Computing*, Vol. 1, pp. 221–242, 2001.
10. J. Zhang, Q. Zhang, B. Li, X. Luo, and W. Zhu, Energy-efficient routing in mobile ad hoc networks: mobility-assisted case, *IEEE Transactions On Vehicular Technology*, Vol. 55, No. 1, pp. 369–379, 2006.

11. A. D. Assouma, R. Beaubrun, and S. Piere, Mobility management in heterogeneous wireless networks, *IEEE Journal on Selected Areas in Communications*, Vol. 24, No. 3, pp. 638–648, 2006.
12. P. N. Pathirana, A. V. Savhin, and S. Jha, Location estimation and trajectory prediction for cellular networks with mobile base stations, *IEEE Transactions on Vehicular Technology*, Vol. 53, No. 6, pp. 1903–1913, 2004.
13. H. Schober, F. Jondral, R. Stirling-Gallacher, and Z. Wang, Adaptive channel estimation for OFDM based high speed mobile communication systems, in *Proc. IEEE International Conference on 3rd Generation Wireless and Beyond*, San Francisco, USA, June 2001, pp. 392–397.
14. R. C. Cannizzaro, P. Banelli, and G. Leus, Adaptive channel estimation for OFDM systems with Doppler spread, in *Proc. IEEE SPAWC'06*, July 2006, pp. 1–5.
15. J. Oh and J. M. Cioffi, Sub-band rate and power control for wireless OFDM systems, in *Proc. IEEE VTC'04*, Sept. 2004, pp. 2011–2014.
16. K. B. Song, A. Ekbal, S. T. Chung, and J. M. Cioffi, Adaptive modulation and coding (AMC) for bit-interleaved coded OFDM (BIC-OFDM), *IEEE Transactions on Wireless Communications*, Vol. 5, No. 7, pp. 1685–1694, 2006.
17. M. D. Austin and G. L. Stuber, Velocity adaptive handoff algorithms for microcellular systems, *IEEE Transactions on Vehicular Technology*, Vol. 43, No. 3, pp. 549–561, 1994.
18. R. Narasimhan and D. C. Cox, Speed estimation in wireless systems using wavelets, *IEEE Transaction on Communications*, Vol. 47, No. 9, pp. 1357–1364, 1999.
19. C. Xiao, K. D. Mann, and J. C. Olivier, Mobile speed estimation for TDMA-based hierachical cellular systems, *IEEE Transactions on Vehicular Technology*, Vol. 50, No. 4, pp. 981–991, 2001.
20. C. Xiao, Estimating velocity of mobiles in EDGE systems, in *Proc. IEEE ICC'02*, Apr. 2002, pp. 3240–3244.
21. G. Azemi, B. Senajij, and B. Boashash, Mobile unit velocity estimation based on the instantaneous frequecny of the received signal, *IEEE Transactions on Vehicular Technology*, Vol. 53, No. 3, pp. 716–724, 2004.
22. L. Zhao and J. W. Mark, Mobile speed estimation based on average fade slope duration, *IEEE Transaction on Communications*, Vol. 52, No. 12, pp. 2066–2069, 2004.
23. G. Park, S. Nam, T. Yu, D. Hong, and C. Kang, A modified covariance-based mobile velocity estimation method for Rician fading channels, *IEEE Communications Letters*, Vol. 9, No. 8, pp. 706–708, 2005.
24. S. Mohanty, VEPSD: a novel velocity estimation algorithm for next-generation wireless systems, *IEEE Transactions on Wireless Communications*, Vol. 4, No. 6, pp. 2655–2660, 2005.
25. K. E. Baddour and N. C. Beaulieu, Robust Doppler spread estimation in nonisotropic fading channels, *IEEE Transactions on Wireless Communications*, Vol. 4, No. 6, pp. 2677–2682, 2005.
26. Y. R. Zheng and C. Xiao, Mobile speed estimation for broadband wireless communications over Rician fading channels, *IEEE Transactions on Wireless Communications*, Vol. 8, pp. 1–5, 2009.
27. H. Schober and F. Jondral, Velocity estimation for OFDM based communication systems, in *Proc. IEEE VTC'02*, Sept. 2002, pp. 715–718.
28. T. Yucek, R. M. A. Tannious, and H. Arslan, Doppler spread estimation for wireless OFDM systems, in *Proc. IEEE/Sarnoff Symposium on Advances in Wired and Wireless Communication*, Apr. 2005, pp. 233–236.
29. J. Cai, W. Song, and Z. Li, Doppler spread estimation for mobile OFDM systems in Rayleigh fading channels, *IEEE Transactions on Consumer Electronics*, Vol. 49, No. 4, pp. 973–977, 2003.
30. A. Doukas and G. Kalivas, Doppler spread estimation in frequency selective Rayleigh channels for OFDM systems, in *Proc. 5th International Symposium in Communication Systems, Networks and Digital Signal Processing*, Patras, Greece, July 2006.
31. A. J. Paulraj, R. Nabar, and D. Gore, *Introduction to Space-Time Wireless Communications*, Cambridge University Press, 2003.
32. C. Xiao, J. Wu, S. Y. Leong, Y. R. Zheng, and K. B. Letaief, A discrete-time model for triply selective MIMO Rayleigh fading channel, *IEEE Transactions on Wireless Communications*, Vol. 3, No. 5, pp. 1678–1688, 2004.
33. Y. R. Zheng and C. Xiao Novel sum-of-sinusoids simulation models for Rayleigh and Rician fading channel, *IEEE Transactions on Wireless Communications*, Vol. 5, No. 12, pp. 3667–3679, 2006.
34. P. A. Bello, Characterization of randomly time-variant linear channels , *IEEE Transactions on Communications Systems*, Vol. 11, No. 4, pp. 360–393, 1963.

Author Biographies

Jun Tao received the B.S. and M.S. degrees from the Department of Radio Engineering, Southeast University, Nanjing, China, in 2001 and 2004, respectively. From 2004 to 2006, he was a system design engineer with Realsil Microelectronics Inc. (a subsidiary of Realtek), Suzhou, China. He is currently pursuing his Ph.D. degree at the Department of Electrical and Computer Engineering, University of Missouri, Columbia, MO, USA. His research interests include channel estimation and equalization for MIMO and OFDM wireless communication systems, and robust receiver design for underwater acoustic communications.

Jingxian Wu received the B.S. degree in Electronic Engineering from Beijing University of Aeronautics and Astronautics, Beijing, China, in 1998, the M.S. degree in Electronic Engineering from Tsinghua University, Beijing, in 2001, and the Ph.D. degree in Electrical Engineering from the University of Missouri, Columbia, in 2005. He is currently an Assistant Professor with the Department of Electrical Engineering, University of Arkansas, Fayetteville. His research interests mainly focus on wireless communications and wireless networks, including ultra-low power wireless communications, cooperative communications, distributed space-time-frequency coding, and cross-layer optimization. Dr. Wu is a member of Tau Beta Pi. He is currently an Associate Editor of the IEEE Transactions on Vehicular Technology. He served as a Cochair for the Wireless Communication Symposium of the 2009 IEEE Global Telecommunications Conference, as a Cochair for the Communication and Information Theory Symposium of the 2010 International Wireless Communications and Mobile Computing Conference, and as a Student Travel Grant Chair for the 2010 IEEE International Conference on Communications. Since 2006, he has

served as a Technical Program Committee Member for a number of international conferences, including the IEEE Global Telecommunications Conference, the IEEE Wireless Communications and Networking Conference, and the IEEE International Conference on Communications.

Chengshan Xiao received the B.S. degree in Electronic Engineering from the University of Electronic Science and Technology of China, Chengdu, China, in 1987, the M.S. degree in Electronic Engineering from Tsinghua University, Beijing, China, in 1989, and the Ph.D. degree in Electrical Engineering from the University of Sydney, Sydney, Australia, in 1997. From 1989 to 1993, he was with the Department of Electronic Engineering, Tsinghua University, where he was on the Research Staff and then became a Lecturer. From 1997 to 1999, he was a Senior Member of Scientific Staff with Nortel, Ottawa, ON, Canada. From 1999 to 2000, he was a Faculty Member with the University of Alberta, Edmonton, AB, Canada. From 2000 to 2007, he was with the University of Missouri, Columbia, where he was an Assistant Professor and then an Associate Professor. He is currently an Associate Professor with the Department of Electrical and Computer Engineering, Missouri University of Science and Technology, Rolla (formerly University of Missouri, Rolla). His research interests include wireless communications, signal processing, and underwater acoustic communications. He is the holder of three U.S. patents. His algorithms have been implemented into Nortel's base station radios with successful technical field trials and network integration. Dr. Xiao is the founding Area Editor for Transmission Technology of the IEEE TRANSACTIONS ON WIRELESS COMMUNICATIONS. Previously, he was an Associate Editor for the IEEE TRANSACTIONS ON VEHICULAR TECHNOLOGY and the IEEE TRANSACTIONS ON CIRCUITS AND SYSTEMS I. He is the lead Technical Program Co-chair of the 2010 IEEE International Conference on Communications (ICC). Previously, he was the lead Co-chair of the 2008 IEEE ICC Wireless Communications Symposium and the Phy/MAC Program Co-chair of the 2007 IEEE Wireless Communications and Networking Conference. He is the founding Chair of the IEEE Communications Society Technical Committee on Wireless Communications.